Hubble tension and matter inhomogeneities: a theoretical perspective

San Martín, Marco, 1 ★ Rubio, Carlos²

¹ Instituto de Astrofísica, Pontificia Universidad Católica de Chile, Avda. Vicuña Mackenna 4860, Santiago 7820436, Chile

Accepted XXX. Received YYY; in original form ZZZ

ABSTRACT

We have studied how local density perturbations could reconcile the Hubble tension. We reproduced a local void through a perturbed FLRW metric with a potential Φ which depends on both time and space. This method allowed us to obtain a perturbed luminosity distance, which is compared with both local and cosmological data. We got a region of local parameters, q_0^{Lo} and j_0^{Lo} , which are in agreement with a local void of $\Omega_{m,\text{void}} = -0.30 \pm 0.15$ explaining the differences between the local H_0 and the Planck H_0 . However, when constraining local cosmological parameters with previous results, we found that neither Λ CDM nor $\Lambda(\omega)$ CDM could solve the Hubble tension.

Key words: Cosmology: theory – cosmological parameters – distance scale

1 INTRODUCTION

Knowledge of cosmology has great importance for the understanding of the physics laws that describe the universe. This is described with the standard model called ΛCDM, which indicates that the universe is mainly composed of radiation, baryonic matter (BM), dark matter (DM), and dark energy (DE) (Perlmutter et al. 1999; Riess et al. 1998; Planck Collaboration et al. 2020).

This model indicates that approximately 5% of the universe is made of baryons 69% DE and 26% DM, but these components are still not completely understood. Despite Λ CDM has been adopted as the standard model to describe the universe at long scales, the improvement in the accuracy of the cosmological parameters has increased the tension with this model, for instance, problems with the curvature compatibility in the Planck data (Valentino et al. 2019) or the Hubble tension (Riess et al. 2016).

In this work, we are interested in study the Hubble tension between the Planck and the local measurements of the Hubble constant (H_0) . Regarding this parameter, the H_0 found by Planck is modeldependent because it requires all the perturbation theory associated with the model. In contrast, the local measurements (Riess et al. 2016, 2018, 2019, 2021) only require a geometrical description of the distance that consider the expansion of the universe and how the flux of photons changes with the distance to the source. It is possible to delete the degeneration between the absolute magnitude of the supernovae Ia (SNe-Ia) and the H_0 considering different calibrations, allowing to find an accurate H_0 value. Many observations has been constraining the H_0 values and claiming this tension with Planck. In general, the local measurements tends to be higher than the Planck H_0 value. For example, Sorce et al. (2012) found a H_0 value of $75.2 \pm 3.0 \text{ km Mpc}^{-1} \text{ s}^{-1}$ based on Sne-Ia. A few years later, Riess et al. (2016) found an observed value $H_0 = 73.24 \pm 1.74$ $km\ Mpc^{-1}\ s^{-1}$ using new parallaxes from Cepheids. This value is 3.4 σ higher than 66.93 \pm 0.62 km Mpc⁻¹ s⁻¹ predicted by Λ CDM

* E-mail: mlsanmartin@uc.cl

with Planck. But the discrepancy reduces to 2.1 σ with respect to the prediction of 69.3 ± 0.7 km Mpc⁻¹ s⁻¹ based on the comparably precise combination of WMAP+ACT+SPT+BAO observations.

This tension between both observations has been widely discussed. For instance, there are different methods to calibrate the SNe-Ia. Regarding the cepheids calibration, the value of H_0 found in (Riess et al. 2018, 2019; Breuval, Louise et al. 2020) is higher than 73 km Mpc⁻¹ s⁻¹, where in the last one publication, Riess et al. (2021) found that H_0 is 73.0 ± 1.4. All these values are far from the H_0 of Planck. However, the calibrations based on TRGB are lower than the cepheids measurements but higher than Planck, (Yuan et al. 2019; Soltis et al. 2021) (72.4 ± 2 and 72.1 ± 2.1 km Mpc⁻¹ s⁻¹, respectively) and Freedman et al. (2019, 2020) found that H_0 is 69.8 ± 1.9 and 69.6 ± 1.9 km Mpc⁻¹ s⁻¹, respectively. These values are lower than the previous based on cepheids but higher than the Planck value. Huang et al. (2020) made a calibration based on Miras and found $H_0 = 73.30 \pm 4$ km Mpc⁻¹ s⁻¹, which is a high value compared with Planck, but also with a big uncertainty.

Many solutions have been proposed to explain this tension, such as extended models based on ΛCDM (Guo et al. 2019), time-varying DE density models (Risaliti & Lusso 2019), or cosmography models (Benetti & Capozziello 2019). Others attempt modifications in the early-time physics, including a component of dark radiation (Bernal et al. 2016) or analyzing early physics related to the sound horizon (Aylor et al. 2019). Many efforts related to recombination physics have been developed to solve the Hubble tension (Agrawal et al. 2019; Lin et al. 2019; Knox & Millea 2020).

This controversy opens a window for new alternative theories based on modifications or variations of ΛCDM such as (Haslbauer et al. 2020; Camarena & Marra 2018; Huang & Wang 2016; Li et al. 2013; Cedeño et al. 2019; Xu et al. 2019; Deser & Woodard 2019; Anagnostopoulos et al. 2019; Poulin et al. 2018; Martín et al. 2021), other proposals introduce modifications in the physics of neutrinos, for example (Battye & Moss 2014; Zhang et al. 2014; Bernal et al. 2016; Valentino & Bouchet 2016; Guo et al. 2017; Feng et al. 2017; Zhao et al. 2017; Guo & Zhang 2017; Benetti et al. 2017; Feng et al.

² Facultad de Ingeniería y Ciencias, Universidad Adolfo Ibañez, Diagonal Las Torres 2640, Peñalolén, Santiago, Chile

2018; Zhao et al. 2018; Benetti et al. 2018; Choudhury & Choubey 2019; Carneiro et al. 2019; Nakamura et al. 2019) and others consider that DE can couple with DM: (Salvatelli et al. 2013; Costa et al. 2014; Yang et al. 2017; Di Valentino et al. 2017b; Feng et al. 2019; Yang et al. 2018).

Some independent studies support the idea that the tension is due more to the physics rather than observational errors (Benetti & Capozziello 2019; Bonvin et al. 2016; Abbott et al. 2018; Lemos et al. 2018). Others have found tension in the CMB analysis (Addison et al. 2016; Valentino et al. 2019) or suggest errors in the values predicted by Planck CMB (Spergel et al. 2015). Also, it has been suggested as a solution to include modifications in the Planck analysis through more free parameters and varying the Equation of State of DE (Di Valentino et al. 2016; Di Valentino et al. 2017a). Also, it has been suggested that changing the cosmic sound horizon, the H_0 tension could be solved, but recently (Jedamzik et al. 2021) has discarded this option because it develops tension with BAOs or galaxy weak lensing data.

In this work, we study the possibility that the local Hubble measurements differ from the Planck data because the local density of the universe is different from the global; in other words, the universe is not sufficiently homogeneous at the scales the SNe-Ia are observed. This idea has been previously studied by Böhringer, Hans et al. (2020); Haslbauer et al. (2020); Keenan et al. (2013); Shanks et al. (2018); Kasai & Futamase (2019); Kenworthy et al. (2019); Cai et al. (2021). In general, they used the Lemaître-Tolman-Bondi (LTB) metric to describe the local void, or studied the influence of the subdensity on the velocities of the galaxies. In this paper, we developed a different approach: we assume a FLRW metric with scalar perturbations in a Newtonian gauge with no curvature to describe an inhomogeneity that is spherically symmetric.

This approach considers the temporal evolution of the field. This evolution is essential because from redshift 0.15 until now elapse approx. 2 Gyrs. This period allows the galaxies to move through space due to the field. In other words, our description allows a local spherically symmetric overdensity/subdensity, which affects the real dependence of the luminosity distance measured by a local observer centered on the origin of this inhomogeneity. This description can be used to describe a local void from a theoretical approach.

Finally, we compare our results with observational evidence of the local void, such as the amplitude of the local underdensity. In the results and conclusions, we comment on the differences between our methods and others.

2 BACKGROUND COSMOLOGY

In this work, we assume that the universe is flat and is composed of radiation, matter (BM and DM), and DE. The flat FLRW metric is given by

$$ds^{2} = -c^{2}dt^{2} + a(t)^{2} \left(dx^{2} + dy^{2} + dz^{2} \right), \tag{1}$$

Using the Einstein field equations

$$G_{\mu\nu} = \kappa T_{\mu\nu},\tag{2}$$

where $\kappa \equiv \frac{8\pi G}{c^4}$ and the definition of a perfect fluid given by

$$T^{\mu\nu} = (\rho + p) u^{\mu} u^{\nu} + p g^{\mu\nu} \tag{3}$$

where ρ is the density and p the pressure of the fluid, we get the Friedmann equation:

$$H^2 \equiv \left(\frac{\dot{a}}{a}\right)^2 = \frac{8\pi G\rho}{3}.\tag{4}$$

The density ρ is determined by all the contributions (m is for matter, which containts baryonic and dark matter):

$$\rho = \frac{3H_0^2}{8\pi G} \left(\frac{\Omega_{r,0}}{a^4} + \frac{\Omega_{m,0}}{a^3} + \Omega_{\Lambda} \right). \tag{5}$$

Also, it is essential to define the density parameter $\Omega_{x,0}$ is associated with the x component of the universe as

$$\Omega_{x,0} = \frac{\rho_{x,0}}{\rho_{c,0}},\tag{6}$$

where ρ_c is the critical density of the universe, and the subscript 0 denotes the parameter evaluated today. Then, the critical density today is $\rho_{c,0} = \frac{8\pi G}{3H_0^2}$, where H_0 is the Hubble constant. We emphasize that in standard cosmology, the dark energy is determined by a constant, but in this work, we work in a generalized case, where Ω_{Λ} depends on time (today the scale factor is defined as $a_0 \equiv 1$).

From the equation (4), the Λ CDM model preserves:

$$\Omega_{r,0} + \Omega_{m,0} + \Omega_{\Lambda,0} = 1,\tag{7}$$

In the following sections, we assume that the DE depends on time, a curvature parameter k = 0, and two different Hubble constants H_0 denoted with different superscripts. The H_0^{Pl} is an acronym for the Planck measurements and H_0^{Lo} indicates Local measurements. In our simplified description of the universe with inhomogeneities, the long distances measurements in cosmology contain information about the mean of the universe, which is mainly flat and without inhomogeneities and anisotropies, as the cosmological principle says. In this scenario, the proper way to describe the universe is the background cosmology given by the standard FLRW metric given in equation (1). If there is a local inhomogeneity, this could be detectable depending on the amplitude of this perturbation. We assume a spherically symmetric inhomogeneity. The metric has no direct effects on the cosmological angular properties (for example, the angular diameter distance d_A), but there are effects on the luminosity distance d_L because the distance traveled by a photon in radial direction changes. This inhomogeneity changes the local physical description of the universe, and then, the properties that an observer measures who assumes a nonperturbed metric are not correct. In this scenario, the Hubble constant measure by the observer who neglects the perturbative effect is given by H^{Lo} , and it is not the real physical expansion rate. If the people use cosmographical models expanding cosmological parameters as a series in time, scale factor, or redshift, and if they assume a non perturbed space, they are finding values that are not comparable with the long distances cosmological parameters (such as the Planck values). The observable measured parameters, which are determined by assuming a nonperturbed FLRW metric, are denoted with the superscript Lo (from local). In this context, an advantageous and common way of expanding the scale factor as a function of $\tau \equiv t - t_0$ and the cosmological parameters H_0 (Hubble constant), q_0 (deceleration parameter) and j_0 (jerk). In our method, we will use two different series with different meanings. a^{Pl} is useful

to describe the universe at a big scale, which has no perturbation terms:

$$a^{\rm Pl}(\tau) \approx 1 + H_0^{\rm Pl}\tau - \frac{1}{2}q_0^{\rm Pl}\left(H\tau\right)^2 + \frac{1}{6}j_0^{\rm Pl}\left(H\tau\right)^3 + O\left(\tau\right)^4, \tag{8}$$

By the other hand, the a^{Lo} expansion describes the local universe, where the perturbations are important:

$$a^{\rm Lo}(\tau) \approx 1 + H_0^{\rm Lo}\tau - \frac{1}{2}q_0^{\rm Lo}\left(H\tau\right)^2 + \frac{1}{6}j_0^{\rm Lo}\left(H\tau\right)^3 + O\left(\tau\right)^4. \tag{9}$$

The *Local* and the *Planck* parameters can coincide only when there is no perturbation. In another case, we have to study if the discrepancy can be explained assuming this perturbation. In the next section, we develop the effects of the perturbative terms in the luminosity distance. We emphasise that we will consider two scenarios, the first is determined by Λ CDM with constant DE and a flat universe, and the second is described by $\Lambda(z)$ CDM in a flat universe. In both cases the series expansions given by equations (8) and (9) has to be consistent with the respective DE fluid equation.

3 PERTURBATION THEORY

We use a perturbed metric assuming the Newtonian Gauge with scalar perturbations represented by $\Psi(t, \vec{x})$ and $\Phi(t, \vec{x})$ in linear perturbation theory. Then, the most general metric is

$$ds^{2} = -c^{2} \left(1 + 2\Phi(t, \vec{x}) \right) dt^{2} + a(t)^{2} \left(1 - 2\Psi(t, \vec{x}) \right) \left(dx^{2} + dy^{2} + dz^{2} \right). \tag{10}$$

As usual, the scalar perturbations are determined by the Bardeen potentials where the vector and tensor perturbations have been defined as 0. Ψ is related to the Newtonian potential, and Φ is associated with the spatial curvature perturbation.

Note that every perturbed quantity will be denoted with a superindex $^{(n)}$, which indicates the order of the perturbation.

We are interested in describing an expanding universe with a local inhomogeneity described by the Bardeen potentials. To describe the universe today, we can neglect the radiation contribution (z < 0.15 Riess et al. (2016)). If the perturbations are caused by matter (BM and DM), then the first-order contribution $T^{\mu\nu}$ can appear as matter density perturbation, but not as a pressure perturbation. In other words, we are neglecting any interaction between matter, such as collisions or merges of galaxies. The DE appears as a constant density and pressure, but without perturbative terms. The perturbed matter term can move through space because it feels the Bardeen potentials which can evolve through time. This implies that the 4-velocity has to be perturbed, where we have included the DE term inside the energy-momentum tensor $T_{\mu\nu} = T_{\mu\nu} - \Lambda g_{\mu\nu}$ and $\kappa = 8\pi G/c^4$.

3.1 Perturbed Einstein equations

We expand the density, pressure and 4-velocity up to first order,

$$\rho \approx \rho^{(0)} + \rho^{(1)},$$
(11)

$$p \approx p^{(0)} + p^{(1)},$$
 (12)

$$u^{\mu} \approx u^{\mu(0)} + u^{\mu(1)}. \tag{13}$$

Using that $g_{\mu\nu}u^{\mu}u^{\nu}=-c^2$ and defining the velocity as (v^x,v^y,v^z) , then

$$u^{\mu} \approx (1 - \Phi, v^x, v^y, v^z), \tag{14}$$

$$u_{\mu} \approx (-c^2(1+\Phi), a^2v^x, a^2v^y, a^2v^z),$$
 (15)

and with the equation (3) we get the perturbed Einstein equations $(\mathbf{G^0}_0{}^{(1)} = \kappa \mathbf{T^0}_0{}^{(1)}, \mathbf{G^i}_0{}^{(1)} = \kappa \mathbf{T^i}_0{}^{(1)}$, and $\mathbf{G^i}_i{}^{(1)} = \kappa \mathbf{T^i}_i{}^{(1)})$

$$3H\dot{\Phi} - \frac{c^2}{a^2}\nabla^2\Phi + 3\Phi H^2 = -4\pi G \rho_m^{(1)},\tag{16}$$

$$(H\partial_i \Phi + \partial_i \dot{\Phi}) = -4\pi G a^2 \rho^{(0)} v^i, \tag{17}$$

$$\Phi\left(3H^2 + 2\dot{H}\right) + 4H\dot{\Phi} + \ddot{\Phi} = 0. \tag{18}$$

As we assume an isotropic fluid, then the equation $i \neq j$ implies that $\Psi = \Phi$. Now, we introduce a velocity potential v^N as $\vec{v} = -\nabla v^N$, then the equations (16)-(18) are

$$\nabla^2 \Phi = 4\pi G a^2 \rho_m^{(1)} + 3H a^2 (H \Phi + \dot{\Phi}), \tag{19}$$

$$H\Phi + \dot{\Phi} = 4\pi G a^2 \rho^{(0)} v^N, \tag{20}$$

$$\Phi \left(3H^2 + 2\dot{H} \right) + 4H\dot{\Phi} + \ddot{\Phi} = 0. \tag{21}$$

3.2 Redshift dependence

Considering the isotropic condition, the perturbed metric in spherical coordinates is

$$ds^{2} = -(1+2\Phi)c^{2}dt^{2} + (1-2\Phi)a^{2}dr^{2} + a^{2}r^{2}d\Omega^{2},$$
 (22)

where the field Φ is spherically symmetric, $|\Phi(t,r)| \ll 1$ and $d\Omega^2 = d\theta^2 + \sin(\theta)^2 d\phi^2$.

To find an expression for the luminosity distance that considers the effects produced by the perturbation, we have to get an expression for the redshift as a function of the perturbations. Imagine a photon emitted at time t_e at distance r_e which is received at the origin at r=0 at t_o . A second photon is emitted at $t_e+\Delta t_e$ and received at $t_o+\Delta t_o$ (e for emitted and o for observed). Both emissions satisfy that $ds^2=0$. If we consider that the trajectory is radial t, then

$$-(1+\Phi)cdt = (1-\Phi)adr. \tag{23}$$

We parametrise the photon trajectory from r_e to r=0 as $\gamma(t)$. We do not require to know the explicit function, $\gamma(t)$ is a function because for every t in the trajectory there is only one position $\gamma(t)$. Furthermore, $\gamma(t)$ is bijective because the light always moves to us. Note that $\gamma(t)$ is the same expression for both trajectories but with different domains and images. In other words, both particles see the same field Φ but different times t and positions t. For both trajectories, we can express $\Phi(t,t)$ as a function of t because, for every photon, the only relevant information is how Φ is when the photon travels along that trajectory. Note that Φ does not change in small scales (Δt_o and Δt_e are small because they are related with frequency). The parametrization of the trajectories for both photons is γ_1 and γ_2 . The beginning and the end of the trajectories are

¹ Note that the minus sign appears because the light travels to us. Then the integration has to be made from $r_e \to 0$ and $t_e \to t_o$. If there is no expansion, then $\frac{-r_e}{t_o-t_e} = -c$.

$$\gamma_1(t_e) = r \tag{24}$$

$$\gamma_1(t_o) = 0, \tag{25}$$

$$\gamma_2(t_e + \Delta t_e) = r \tag{26}$$

$$\gamma_2(t_o + \Delta t_o) = 0. (27)$$

Using this parametrisation, the Φ potential can be written as a function of the time. Then, applying the equation (23) to both trajectories (linear order), we get

$$\int_{r_e}^{0} dr = -c \int_{t_e}^{t_o} \frac{1 + 2\Phi(t, \gamma_1(t))}{a(t)} dt + O(\Phi^2), \tag{28}$$

$$\int_{r_e}^{0} dr = -c \int_{t_e + \Delta t_e}^{t_o + \Delta t_e} \frac{1 + 2\Phi(t, \gamma_2(t))}{a(t)} dt + O(\Phi^2). \tag{29}$$

Subtracting both equations, we get

$$\int_{t_{e}}^{t_{o}} \frac{1 + 2\Phi(t, \gamma_{1}(t))}{a(t)} dt - \int_{t_{e}}^{t_{o}} \frac{1 + 2\Phi(t, \gamma_{2}(t))}{a(t)} dt = \int_{t_{o}}^{t_{o} + \Delta t_{o}} \frac{1 + 2\Phi(t, \gamma_{2}(t))}{a(t)} dt - \int_{t_{e}}^{t_{e} + \Delta t_{e}} \frac{1 + 2\Phi(t, \gamma_{2}(t))}{a(t)} dt.$$
(30)

In contrast with the standard derivation of the redshift, the first two integrals are different because $\gamma_1 \neq \gamma_2$. In both integrals the field Φ is evaluated at time t, and the difference occurs in the position where it is evaluated. If we choose $\delta t = \max{\{\Delta t_O, \Delta t_e\}}$, such as δt is the biggest difference in time considering $t \in (t_e, t_O)$, then $|\gamma_2(t+\delta t)-\gamma_2(t)| \sim c\delta t \approx \lambda$, because $\delta t \approx 1/\nu$. Therefore, in the most extreme case $\Phi(t,\gamma_2(t))$ and $\Phi(t,\gamma_1(t))$ are shifted by a distance λ . We assume that Φ is constant at λ scale which is reasonable. Then the first two integrals can be neglected. Note that with this consideration $\Phi(t,\gamma_2(t)) \approx \Phi(t,\gamma_1(t))$, then

$$\int_{t_o}^{t_o + \Delta t_o} \frac{1 + 2\Phi(t, \gamma_1(t))}{a(t)} dt = \int_{t_e}^{t_e + \Delta t_e} \frac{1 + 2\Phi(t, \gamma_1(t))}{a(t)} dt, \quad (31)$$

$$(1 + 2\Phi(t_o, \gamma_1(t_o))) \frac{\Delta t_o}{a(t_o)} = (1 + 2\Phi(t_e, \gamma_1(t_e))) \frac{\Delta t_e}{a(t_e)}. \tag{32}$$

Now, we define the redshift as usual,

$$z = \frac{\lambda_o - \lambda_e}{\lambda_e} = \frac{\Delta t_o}{\Delta t_e} - 1 = \frac{\nu_e}{\nu_o} - 1.$$
 (33)

Then, replacing equations (24) and (25) in (33) at linear order we get

$$1 + z = \frac{1 + 2\Phi(t, r) - 2\Phi(t_0, 0)}{a(t)}.$$
 (34)

Note that this approximation does not change if we use γ_1 or γ_2 because Φ is insensitive to scales of λ . We also emphasise that the cosmic time range corresponding to $z \in (0,0.15)$ is $t \in (13.721,11.821)$ Gyrs (using $H_0 \approx 69.6$ Mpc/(km s), $\Omega_{m,0} = 0.286$ in a flat universe). This time range allows Φ to vary. Φ evolves with the time, but it is always spherically symmetric. The time evolution is only produced by the movements of the galaxies in the perturbed metric. We are neglecting anisotropic effects, merging processes, and any other non-ideal effect. This is a simple approach.

3.3 Angular distance

Consider a light source of size D at $r = r_1$ and $t = t_1$ subtending an angle $\delta\theta$ at the origin $(r = 0, t = t_0)$. The proper distance D between the two ends of the object is related to $\delta\theta$ by,

$$D = a(t)rd\theta, (35)$$

then the angular distance $d_A(z)$ is given by the usual expression:

$$d_A(z) = \frac{r(z)}{(1+z)}. (36)$$

There is no change in the angular distance expression with respect to the standard cosmology because the Φ perturbation does not appear in the angular part of the metric.

3.4 Luminosity distance

We followed the standard derivation. A source of light emits photons of energy $h\nu_e$ during a time Δt_e and the observer measures photons with energy $h\nu_o$ during a time Δt_o . Then the power observed is

$$P_o = \frac{h\nu_o}{\Delta t_o}. (37)$$

Using the equation (33) it follows

$$P_o = \frac{h\nu_e}{\Delta t_e} \frac{1}{(1 + z_e)^2}. (38)$$

Finally, using the definition of the emitted power, then the flux F measured on a sphere of radius l is given by

$$F = \frac{L}{4\pi l^2},\tag{39}$$

where dl is determined by a measured made by the observer at time t_O . Then, following the same steps as in the standard cosmology, where dt = 0 implies that the distance today is given by the spatial part evaluated at $t = t_O$

$$l(r) = \int_{o}^{l(r)} dl = a(t_o) \int_{0}^{r} dr = a_o r,$$
(40)

then, in the perturbed metric

$$l(r) = \int_{0}^{l(r)} dl = a(t_0) \int_{0}^{r} \sqrt{1 - 2\Phi(t_0, r)} dr.$$
 (41)

This is the first difference introduced by the potential $\Phi(r)$. Then, the flux measured by the observer is

$$F = \frac{h\nu_e}{\Delta t_e} \frac{1}{4\pi \left(a(t_o) \int_0^{r_e} \sqrt{1 - 2\Phi(t_o, r)} dr \right)^2} \frac{1}{(1 + z_e)^2}.$$
 (42)

Finally, the luminosity distance is defined such that $F \equiv \frac{L}{4\pi d_L^2}$, then

$$d_L(z) = (1+z) \int_0^r \sqrt{1 - 2\Phi(t_0, r)} dr,$$
(43)

where we considered that $a_o = 1$ and the equation (34). Note that

if $\Phi(r) = 0$, the standard definition is recovered. Furthermore, we can expand at first order in Φ

$$d_L(z) = (1+z) \int_0^r (1 - \Phi(t_o, r)) dr + O(\Phi^2), \tag{44}$$

The luminosity distance has changed, but the angular distance has not. The symmetry of the metric produces this.

4 PERTURBED LUMINOSITY DISTANCE

In this section, we will explain in detail the procedure of the expansions that we used to solve the potential $\Phi(t, r)$. It is very important to remark that every element in the expansions is of the order of the perturbation Φ . So, in every step, we linearised our solutions.

4.1 F(t)

First, we separated the potential in temporal and radial parts, F(t) and G(r),

$$\Phi(\tau, r) \equiv F(\tau)G(r), \tag{45}$$

$$F(t) \equiv \Phi_0 + f_1 \tau + f_2 \tau^2 + f_3 \tau^3 + f_4 \tau^4 + O\left(\tau^5\right), (46)$$

$$G(r) \equiv 1 + g_2 r^2 + g_4 r^4 + O(r^6). \tag{47}$$

The units of the coefficients are $[f_i] = s^{-i}$, $[g_i] = \mathrm{Mpc}^{-i}$ and Φ_0 is dimensionless. The equation (47) preserves spherical symmetry. More important, any function G(r) that has this symmetry could be expanded as equation (47), so our election for G(r) at this level is completely general. For our decomposition of $\Phi(t,r)$, we can solve for F(t) using equation (18),

$$F(t)\left(3H^{2}(t)+2\dot{H}(t)\right)+4H(t)\dot{F}(t)+\ddot{F}(t)=0\,. \tag{48}$$

Replacing the equations (8) and (46) in equation (48), we get

$$f_{2} = \frac{1}{2} \left(-f_{0}H_{0}^{Pl^{2}} - 4f_{1}H_{0}^{Pl} + 2f_{0}H_{0}^{Pl^{2}}q_{0}^{Pl} \right) , \qquad (49)$$

$$f_{3} = \frac{1}{6} \left(6f_{0}H_{0}^{Pl^{3}} + 19f_{1}H_{0}^{Pl^{2}} - 2f_{0}H_{0}^{Pl^{3}}j_{0}^{Pl} \right)$$

$$- 8f_{0}H_{0}^{Pl^{3}}q_{0}^{Pl} + 6f_{1}H_{0}^{Pl^{2}}q_{0}^{Pl} \right) , \qquad (50)$$

$$f_{4} = \frac{1}{24} \left(10f_{0}H_{0}^{Pl^{4}}j_{0}^{Pl} + 20f_{0}H0^{PL^{4}}q_{0}^{Pl^{2}} \right)$$

$$+ 30f_{0}H_{0}^{Pl^{4}}q_{0}^{Pl} - 37f_{0}H_{0}^{Pl^{4}} - 8f_{1}H_{0}^{Pl^{3}}j_{0}^{Pl}$$

$$- 76f_{1}H_{0}^{Pl^{3}}q_{0}^{Pl} - 108f_{1}H_{0}^{Pl^{3}} \right) , \qquad (51)$$

with f_0 and f_1 as free parameters (initial conditions), because (48) is a second order equation.

4.2 $\tau(r)$

We need to know how the time is related with the space for photons. To do that, we considered the radial trajectory given by equation (23). In the next step, we expanded the cosmological time as

$$\tau(r) = \tau_1 \left(\frac{r}{c}\right) + \tau_2 \left(\frac{r}{c}\right)^2 + \tau_3 \left(\frac{r}{c}\right)^3 + \tau_4 \left(\frac{r}{c}\right)^4 + \tau_5 \left(\frac{r}{c}\right)^5 + O(r)^6 \ . \tag{52}$$

The units of τ_i are s^{-i+1} . Now we used equation (23) to find the coefficients τ_i . We wrote them in the Appendix.

4.3 Luminosity Distance Expansion

With $\tau(r)$ for photons, we can find the expression for r(z), where z is the redshift. This allows us to integrate the luminosity distance shown in equation (44). With the equation (52), the coefficients f_i from equations (49), (50) and (51), we can find an expression for r(z) using equation (34):

$$r(z) = \frac{cz}{H_0^{\text{Pl}}} \left[\left(1 + \frac{2f_1}{H_0^{\text{Pl}}} \right) + z \left(-\frac{2c^2 f_0 g_2}{H_0^{\text{Pl}^2}} - \frac{3f_1 q_0^{\text{Pl}}}{H_0^{\text{Pl}}} \right) \right.$$

$$+ \frac{2f_1}{H_0^{\text{Pl}}} - 2f_0 q_0^{\text{Pl}} + f_0 - \frac{q_0^{\text{Pl}}}{2} - \frac{1}{2} \right)$$

$$+ z^2 \left(\frac{2c^2 f_1 g_2}{H_0^{\text{Pl}^3}} + \frac{4c^2 f_0 g_2 q_0^{\text{Pl}}}{H_0^{\text{Pl}^2}} + \frac{2c^2 f_0 g_2}{H_0^{\text{Pl}^2}} - \frac{42f_1 j_0^{\text{Pl}}}{3H_0^{\text{Pl}}} \right.$$

$$+ \frac{5f_1 q_0^{\text{Pl}^2}}{H_0^{\text{Pl}}} + \frac{f_1}{3H_0^{\text{Pl}}} - \frac{2f_0 j_0^{\text{Pl}}}{3} + 4f_0 q_0^{\text{Pl}^2}$$

$$- \frac{2f_0 q_0^{\text{Pl}}}{3} - \frac{j_0^{\text{Pl}}}{6} + \frac{q_0^{\text{Pl}^2}}{2} + \frac{2q_0^{\text{Pl}}}{3} + \frac{1}{3} \right) \left. \right] + O(z)^4 . \quad (53)$$

Finally, using the luminosity distance defined in equation (44) we found

$$d_L(z) = \frac{cz}{H_0^{\text{Pl}}} \left(\mathcal{D}_L^0 + \mathcal{D}_L^1 z + \mathcal{D}_L^2 z^2 + O(z)^3 \right), \tag{54}$$

with

$$\mathcal{D}_L^0 = 1 + f_0 + \frac{2f_1}{H_0^{\text{Pl}}}, \tag{55}$$

$$\mathcal{D}_{L}^{1} = \frac{H_{0}^{\text{Pl}} + 6f_{1}}{2H_{0}^{\text{Pl}}} \left(1 - q_{0}^{\text{Pl}}\right) - \frac{4c^{2}f_{0}g_{2}}{2H_{0}^{\text{Pl}^{2}}} + \frac{1}{2}(3 - 5q_{0}^{\text{Pl}}), \quad (56)$$

$$\begin{split} \mathcal{D}_{L}^{2} &= \frac{-1 - j_{0}^{\text{Pl}} + q_{0}^{\text{Pl}} + 3q_{0}^{\text{Pl}^{2}}}{6} + \frac{2c^{2}f_{1}g_{2}}{H_{0}^{\text{Pl}^{3}}} \\ &+ \frac{f_{1}}{3H_{0}^{\text{Pl}}} \left(4 - 4j_{0}^{\text{Pl}} - 6q_{0}^{\text{Pl}} + 15q_{0}^{\text{Pl}^{2}} \right) + \frac{c^{2}f_{0}g_{2}}{3H_{0}^{\text{Pl}^{2}}} \left(1 + 12q_{0}^{\text{Pl}} \right) \end{split}$$

$$+ \frac{f_0}{6} \left(3 - 5j_0^{\text{Pl}} - 11q_0^{\text{Pl}} + 27q_0^{\text{Pl}}^2 \right). \tag{57}$$

This expansion allow us to compare with local expansion of luminosity distance used by Riess et al. (2016). The standard expansion for $d_x^{\rm Std}$ is

$$d_L^{\text{Std}}(z) = \frac{cz}{H_0^{\text{Lo}}} \left(\mathcal{D}_L^{0,\text{Std}} + \mathcal{D}_L^{1,\text{Std}} z + \mathcal{D}_L^{2,\text{Std}} z^2 + O(z)^3 \right), \tag{58}$$

with

$$\mathcal{D}_L^{0,\text{Std}} = 1, \tag{59}$$

$$\mathcal{D}_L^{1,\text{Std}} = -\frac{1}{2}(-1 + q_0^{\text{Lo}}), \tag{60}$$

$$\mathcal{D}_L^{2,\text{Std}} = -\frac{1}{6} (1 - q_0^{\text{Lo}} - 3q_0^{\text{Lo}^2} + j_0^{\text{Lo}}). \tag{61}$$

Comparing equations (55)-(57) with equations (59)-(61) allow us to find the parameters f_0 , f_1 and g_2 as a function of H_0^{Lo} , q_0^{Lo} and

5 MATTER PERTURBATION

5.1 Equation for the matter inhomogeneity

Now that we know $\Phi(t,r)$ in terms of H_0^{Lo} , q_0^{Lo} and j_0^{Lo} (with H_0^{Pl} , $q_0^{\rm Pl}$, and $j_0^{\rm Pl}$ fixed), we can get an expression for the perturbation of matter density, which we can associate to the local void. Let us explicit how. Replacing equation (20) in equation (19) we got

$$c^2 \nabla^2 \Phi = 4\pi G a^2 \rho_m^{(1)} + 3H a^2 (H\Phi + \dot{\Phi}).$$
 (62)

Then

$$\rho_m^{(1)} = \frac{c^2 \nabla^2 \Phi}{4\pi G a^2} - \frac{3H^2 \Phi - 3H\dot{\Phi}}{4\pi G} \,, \tag{63}$$

where the Laplacian in spherical coordinates is given by

$$\nabla^2 f(r) = \frac{1}{r^2} \frac{d}{dr} \left(r^2 \frac{d}{dr} f(r) \right). \tag{64}$$

Replacing $\Phi(t, r) = F(t)G(r)$ in equation (63), gives us the solution for $\rho_m^{(1)}$

$$\rho_m^{(1)}(\tau, r) = \frac{3H^2(\tau)F(\tau) - 3H(\tau)\dot{F}(\tau)}{4\pi G}G(r) + \frac{6c^2\nabla^2G(r)F(\tau)}{4\pi Ga(\tau)^2},$$
(65)

where $\tau = t - t_0$. Evaluating in the present $(\tau = 0)$

$$\rho_m^{(1)}(0,r) = \frac{6c^2\nabla^2 G(r)f_0}{4\pi G} - \frac{3H_0^2 f_0 - 3H_0 f_1}{4\pi G}G(r). \tag{66}$$

5.2 Profile of the void

Up to now, we have said anything about g_4 , this is because in the procedure of section 4, it is a free parameter. Nevertheless, the expansion of equation (47) is only valid for the purpose of finding a series expansion of angular distance. For instance, if we want to describe a general profile, we need to expand G(r) to higher orders:

$$G(r) = \sum_{i=0}^{n} g_{2i} r^{2i} . (67)$$

In order to know every parameter g_{2i} with respect to the parameters in the luminosity distance q_0 , j_0 , s_0 and higher order terms, those cosmological parameters have to be valid to redshift lower than z = 0.15 to keep our procedure in agreement with SNe-Ia local measurements. However, at low redshift those cosmological parameters can not be measured because of a lack of precision in the fits. This insufficient in the precision emerges because at our regime in redshift, powers of z are too smalls. Then, the deviation of these parameters tends to be large, see for instance (Capozziello et al. 2019). Hence, we can not find the parameters g_{2i} as a function of q_0 , j_0 , s_0 and next order parameters. This does not imply that there is no density profile that can satisfy or not the Hubble tension. There is simply no data to assert or reject our hypothesis of a general function G(r). On the other hand, we can consider a simple Gaussian G(r) = $\exp(-\alpha r^2)$ as our hypothesis, then we only need g_2 to determine completely the profile, because in the expansion of G(r) we have $\alpha = -g_2$. The main problem of this approach is that in the expansion shown in equation (47), we cannot cut the series at any order because the complete Gaussian has to be valid for the scale of usual voids ($\sim 300 - 600$ Mpc), or in terms of the redshift: $z \sim 0.15$.

6 RESULTS

Our method found constraints for the local matter perturbation as a function of q_0^{Lo} and j_0^{Lo} . We emphasise that the results depend on the background, then the plots could change if the background cosmology changes (obtained from Planck). In this method, we have assumed that Λ CDM is the correct model. In this case, q_0^{Pl} depends on the DE and matter parameters:

$$q_0^{\rm Pl} = \frac{1}{2} \Omega_{m,0}^{\rm Pl} - \Omega_{\Lambda}^{\rm Pl}. \tag{68}$$

With the Planck Collaboration et al. (2020) data, we fixed $q_0^{\rm Pl}$ = -0.5275. Regarding the second parameter, we assumed that $j_0^{Pl} = 1$ as ACDM predicts.

We also defined a cosmological parameter that represents the size of the matter perturbation with respect to the critical density given by the background cosmology (defined by Planck Collaboration et al. (2020)). This parameter is defined as

$$\Omega_{m,0}^{(1)} = \frac{\rho_m^{(1)}(r=0)}{\rho_{c,0}}.$$
 (69)

We show the results in three plots that summarise the dependence of Φ_0 , $\Omega_{m,0}^{(1)}$ and g_2 with the cosmological parameters q_0^{Lo} and j_0^{Lo} . We did not include the plots based on extended DE model $\Lambda(\omega)$ CDM, because this extended model produced similar plots. We based our calculations on this modified model where the DE fluid equation is extended as $w(a) = w_0 + (1 - a)w_a$, where $w = p_{DE}/\rho_{DE}$ (for more details, see (Planck Collaboration et al. 2020, section 7.4.1)). We include the $\Lambda(\omega)$ CDM plots in notebooks in the section 7.

The Fig. 1 shows Φ_0 as a function of q_0^{Lo} and j_0^{Lo} . The grey zone corresponds to: prohibited solutions (the solutions are not reals), $\Phi_0 > 0.1$, $\Phi_0 < 0$, $g_2 > 0$, $\Omega_{m,0}^{(1)} > -0.15$, and $\Omega_{m,0}^{(1)} < -0.45$. The constraints related with the Φ_0 has been chose to keep Φ_0 as a perturbation, in physics language $|\Phi_0| \ll 1$. This is an arbitrary constraint. Furthermore, we have imposed that Φ_0 must be positive, because we know from the observations we are in a cosmic void. (). Also, we include another constraint on the $\Omega_{m,0}^{(1)}.$ This inhomogeneity must describe a void with about 30%(±)15% of lacking matter Keenan et al. (2013); Böhringer, Hans et al. (2020); Lombriser (2020); Wu & Huterer (2017). The allowed zone shows that q_0^{Lo} is very well constrained between -0.25 and -0.6, approximately. This not happens with j_0^{Lo} , which can take values less than ~ 1.5 . Note that the background values: $q_0^{\text{Pl}} = -0.5275$ and $j_0^{\text{Pl}} = 1$, are forbidden in this scenario; there is no solution at $(q_0^{\text{Lo}}, j_0^{\text{Lo}}) = (-0.5275, 1)$. This also happens in the case of $\Lambda(\omega)$ CDM.

The Fig. 2 shows $\Omega_{m,0}^{(1)}$ as a function of q_0^{Lo} and j_0^{Lo} . The constrains for this plots are the same as in Fig. 1. If the constraints on the matter subdensity are accurate, then the $q_0^{\rm Lo}$ parameter can be very well constrained. This not occurs with $j_0^{\rm Lo}$. However if $j_0^{\rm Lo}$

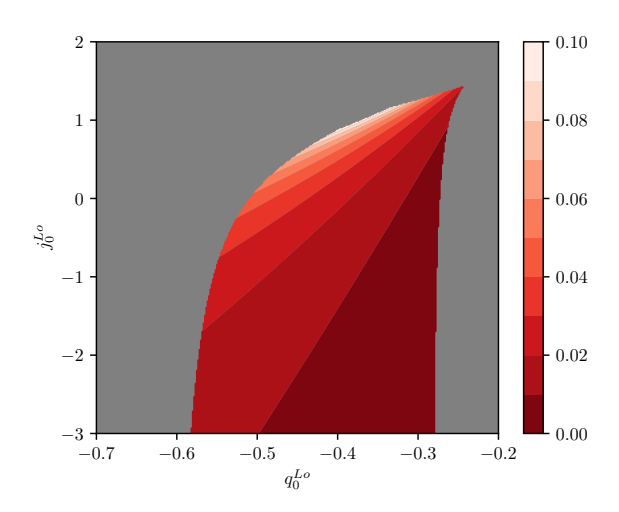


Figure 1. The color shows how Φ_0 depends with on local parameters, $q_0^{\rm Lo}$ and $j_0^{\rm Lo}$. The grey zone is prohibited by: complex solutions, $\Phi_0 > 0.1$, $\Phi_0 < 0$, $g_2 > 0$, $\Omega_{m,0}^{(1)} > -0.15$, and $\Omega_{m,0}^{(1)} < -0.45$.

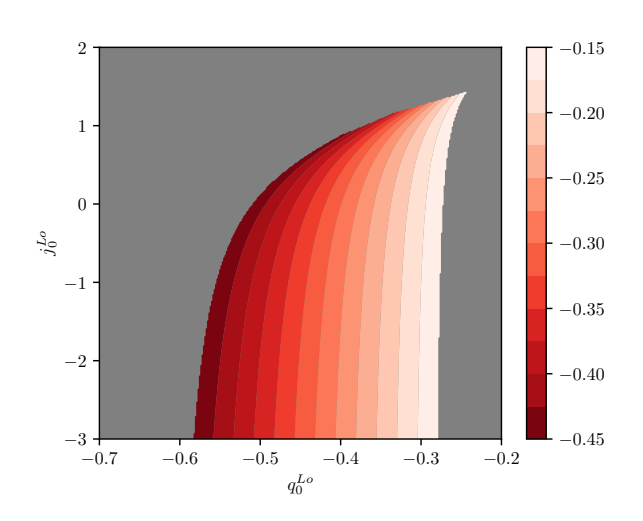


Figure 2. The color shows how $\Omega_{m,0}^{(1)}$ depends on two local parameters, q_0^{Lo} and j_0^{Lo} . The grey zone is prohibited by: complex solutions, $\Phi_0 > 0.1$, $\Phi_0 < 0$, $g_2 > 0$, $\Omega_{m,0}^{(1)} > -0.15$, and $\Omega_{m,0}^{(1)} < -0.45$.

want to be preserved as the same of the background, then the model is strongly constrained, and it only allows a small zone close to $(q_0^{\text{Lo}}, j_0^{\text{Lo}}) = (-0.25, 1)$. This plot is important, because any observational measurement on the local mass density (Böhringer, Hans et al. 2020; Lombriser 2020; Wu & Huterer 2017) constraints the possibilities on the plot, and can discard Λ CDM and $\Lambda(\omega)$ CDM. Nevertheless, the cosmological parameters has to be measured locally, for redshift z < 0.15 (the smaller the better). If we assume 30% of subdensity as a correct local measurement, then q_0^{Lo} tensions with the Capozziello et al. (2019) $(q_0 < -0.6$ for $z \sim 0.1$).

The Fig. 3 shows g_2 as a function of q_0^{Lo} and j_0^{Lo} . In this case, g_2 is always negative, which is a good description of the model. This parameter indicates that the local potential tends to decrease with

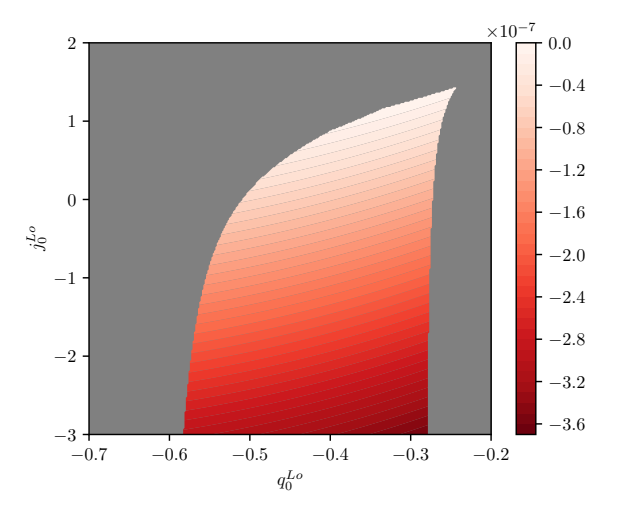


Figure 3. The color shows how g_2 depends on two local parameters, q_0^{Lo} and j_0^{Lo} . The grey zone is prohibited by: complex solutions, $\Phi_0 > 0.1$, $\Phi_0 < 0$, $g_2 > 0$, $\Omega_{m,0}^{(1)} > -0.15$, and $\Omega_{m,0}^{(1)} < -0.45$.

the radius from Φ_0 to $\Phi_0 + g_2 r^2 + ...$ When r increases, $\Phi(r) \to 0$. Nevertheless, we recall that we don't know the higher derivatives of this expansion.

7 CONCLUSIONS

We have showed how local density perturbations could reconcile the Hubble tension between local and cosmological measurements of the Universe expansion. To do this, we perturbed FLRW metric with a potential Φ which varies both in time and space. The temporal evolution is important because from redshift z=0.15 until now elapse approx 2 Gyrs. This is enough time for photons to feel the temporal evolution of the potential due to the local void.

With this perturbation, we have computed the local luminosity distance, which depends on $H_0^{\rm LO}$, $q_0^{\rm LO}$ and $j_0^{\rm LO}$, and we compared it with the cosmological luminosity distance, that depends on $H_0^{\rm Pl}$, $q_0^{\rm Pl}$ and $j_0^{\rm Pl}$. Due to our hypothesis about $\Phi(t,r)$, we could find a region of $q_0^{\rm LO}$ and $j_0^{\rm LO}$ which allow us to explain the variation between $H_0^{\rm LO}$ and $H_0^{\rm Pl}$.

This region of parameters was constrained such that the local density was $\Omega_m = -0.3 \pm 0.15$, in agreement with Keenan et al. (2013), Kasai & Futamase (2019) and Böhringer, Hans et al. (2020). The range of values for Φ_0 in our region is $0 < \Phi_0 < 0.1$. Moreover, an important subset of this region contains enough small Φ_0 values such that the perturbative treatment has physical sense.

It is crucial to point out that our complete region of $q_0^{\rm Lo}$ and $j_0^{\rm Lo}$ is in agreement with Riess et al. (2016) results at redshift z < 0.15; because the local luminosity distance is insensitive to higher order terms, such as $q_0^{\rm Lo}$ and $j_0^{\rm Lo}$ that we explored in this work.

We want to emphasize that our scenario is different from previous studies where the inhomogeneity is described as a contribution in the spatial curvature of the FLRW metric through the LTB metric. In these studies Cai et al. (2021); Kenworthy et al. (2019) the conclusion strengths that the tension on Hubble constant cannot be saved by a local void. Conversely, we worked in the Newtonian gauge for the standard perturbed FLRW metric (the same perturbed metric as in

the CMB Weinberg (2008); Piattella (2018)) and not the LTB metric, finding a suitable region where the local void is enough to explain the differences between local and cosmological Hubble parameter. On the other hand, the idea of that local underdensities can be the origin of the Hubble discrepancy has also been studied using nonlinear evolution (Lombriser 2020; Wu & Huterer 2017), where the underdensities needed are extreme ($\delta_m \approx -0.8$ and -0.5 respectively). Böhringer, Hans et al. (2020) studied the local underdensity through the CLASSIX galaxy cluster survey. They found that part of the H_0 discrepancy can be explained with the local underdensity which was determined as a void of $\delta_m - 30 \pm 15\%$ ($-20 \pm 10\%$) in a region with a radius of about 100 (~ 140) Mpc. Our finding showed that the Hubble tension can be solved for this range of underdensities. Nevertheless, if we compare ours allowed parameters with the Capozziello et al. (2011) and Capozziello et al. (2019) results, where they studied scenarios like $\Lambda(\omega)$ CDM, there is no possible solution to the Hubble tension.

ACKNOWLEDGEMENTS

The author CR thanks to Proyecto Ingeniería 2030 de CORFO número 14ENI2-26865.

DATA AVAILABILITY

The notebooks with the analytical and numerical analysis for Λ CDM and $\Lambda(\omega)$ CDM models are available on GitHub.

REFERENCES

- Abbott T. M. C., et al., 2018, Monthly Notices of the Royal Astronomical Society, 480, 3879
- Addison G. E., Huang Y., Watts D. J., Bennett C. L., Halpern M., Hinshaw G., Weiland J. L., 2016, The Astrophysical Journal, 818, 132
- Agrawal P., Cyr-Racine F.-Y., Pinner D., Randall L., 2019, arXiv e-prints, p. arXiv:1904.01016
- Anagnostopoulos F. K., Benisty D., Basilakos S., Guendelman E. I., 2019, Journal of Cosmology and Astroparticle Physics, 2019, 003
- Aylor K., Joy M., Knox L., Millea M., Raghunathan S., Wu W. L. K., 2019, The Astrophysical Journal, 874, 4
- Battye R. A., Moss A., 2014, Phys. Rev. Lett., 112, 051303
- Benetti M., Capozziello S., 2019, Journal of Cosmology and Astroparticle Physics, 2019, 008
- Benetti M., Graef L. L., Alcaniz J. S., 2017, Journal of Cosmology and Astroparticle Physics, 2017, 003
- Benetti M., Graef L. L., Alcaniz J., 2018, Journal of Cosmology and Astroparticle Physics, 2018, 066
- Bernal J. L., Verde L., Riess A. G., 2016, Journal of Cosmology and Astroparticle Physics, 2016, 019
- Böhringer, Hans Chon, Gayoung Collins, Chris A. 2020, A&A, 633, A19 Bonvin V., et al., 2016, Monthly Notices of the Royal Astronomical Society, 465, 4914
- Breuval, Louise et al., 2020, A&A, 643, A115
- Cai R.-G., Ding J.-F., Guo Z.-K., Wang S.-J., Yu W.-W., 2021, Phys. Rev. D, 103, 123539
- Camarena D., Marra V., 2018, Phys. Rev. D, 98, 023537
- Capozziello S., Lazkoz R., Salzano V., 2011, Phys. Rev. D, 84, 124061
- Capozziello S., Ruchika Sen A. A., 2019, Monthly Notices of the Royal Astronomical Society, 484, 4484
- Carneiro S., de Holanda P. C., Pigozzo C., Sobreira F., 2019, Phys. Rev. D, 100, 023505
- Cedeño F. X. L., Montiel A., Hidalgo J. C., German G., 2019, Journal of Cosmology and Astroparticle Physics, 2019, 002

- Choudhury S. R., Choubey S., 2019, The European Physical Journal C, 79Costa A. A., Xu X.-D., Wang B., Ferreira E. G. M., Abdalla E., 2014, Phys. Rev. D, 89, 103531
- Deser S., Woodard R., 2019, Journal of Cosmology and Astroparticle Physics, 2019, 034
- Di Valentino E., Melchiorri A., Silk J., 2016, Physics Letters B, 761, 242
- Di Valentino E., Melchiorri A., Linder E. V., Silk J., 2017a, Phys. Rev. D, 96, 023523
- Di Valentino E., Melchiorri A., Mena O., 2017b, Phys. Rev. D, 96, 043503
- $Feng\ L., Zhang\ J.-F., Zhang\ X., 2017, \\ The\ European\ Physical\ Journal\ C, 77$
- Feng L., Zhang J.-F., Zhang X., 2018, Science China Physics, Mechanics & Astronomy, 61
- Feng L., Zhang J.-F., Zhang X., 2019, Physics of the Dark Universe, 23, 100261
- Freedman W. L., et al., 2019, The Astrophysical Journal, 882, 34
- Freedman W. L., et al., 2020, The Astrophysical Journal, 891, 57
- Guo R.-Y., Zhang X., 2017, The European Physical Journal C, 77
- Guo R.-Y., Li Y.-H., Zhang J.-F., Zhang X., 2017, Journal of Cosmology and Astroparticle Physics, 2017, 040
- Guo R.-Y., Zhang J.-F., Zhang X., 2019, Journal of Cosmology and Astroparticle Physics, 2019, 054
- Haslbauer M., Banik I., Kroupa P., 2020, Monthly Notices of the Royal Astronomical Society, 499, 2845–2883
- Huang Q.-G., Wang K., 2016, The European Physical Journal C, 76
- Huang C. D., et al., 2020, The Astrophysical Journal, 889, 5
- Jedamzik K., Pogosian L., Zhao G.-B., 2021, Communications Physics, 4
- Kasai M., Futamase T., 2019, Progress of Theoretical and Experimental Physics, 2019
- Keenan R. C., Barger A. J., Cowie L. L., 2013, The Astrophysical Journal, 775, 62
- Kenworthy W. D., Scolnic D., Riess A., 2019, The Astrophysical Journal,
- Knox L., Millea M., 2020, Phys. Rev. D, 101, 043533
- Lemos P., Lee E., Efstathiou G., Gratton S., 2018, Monthly Notices of the Royal Astronomical Society, 483, 4803
- Li M., Li X.-D., Ma Y.-Z., Zhang X., Zhang Z., 2013, Journal of Cosmology and Astroparticle Physics, 2013, 021
- Lin M.-X., Benevento G., Hu W., Raveri M., 2019, Phys. Rev. D, 100, 063542 Lombriser L., 2020, Physics Letters B, 803, 135303
- Martín M. S., Alfaro J., Rubio C., 2021, The Astrophysical Journal, 910, 43Nakamura S., Kase R., Tsujikawa S., 2019, Journal of Cosmology and Astroparticle Physics, 2019, 032
- Perlmutter S., et al., 1999, The Astrophysical Journal, 517, 565
- Piattella O. F., 2018, Lecture Notes in Cosmology. UNITEXT for Physics, Springer, Cham (arXiv:1803.00070), doi:10.1007/978-3-319-95570-4
- Planck Collaboration et al., 2020, A&A, 641, A6
- Poulin V., Boddy K. K., Bird S., Kamionkowski M., 2018, Phys. Rev. D, 97, 123504
- Riess A. G., et al., 1998, Astron.J., 116, 1009
- Riess A. G., et al., 2016, The Astrophysical Journal, 826, 56
- Riess A. G., et al., 2018, The Astrophysical Journal, 855, 136
- Riess A. G., Casertano S., Yuan W., Macri L. M., Scolnic D., 2019, The Astrophysical Journal, 876, 85
- Riess A. G., Casertano S., Yuan W., Bowers J. B., Macri L., Zinn J. C., Scolnic D., 2021, The Astrophysical Journal, 908, L6
- Risaliti G., Lusso E., 2019, Nature Astronomy, 3, 272–277
- Salvatelli V., Marchini A., Lopez-Honorez L., Mena O., 2013, Phys. Rev. D, 88, 023531
- Shanks T., Hogarth L. M., Metcalfe N., 2018, Monthly Notices of the Royal Astronomical Society: Letters, 484, L64
- Soltis J., Casertano S., Riess A. G., 2021, The Astrophysical Journal Letters,
- Sorce J. G., Tully R. B., Courtois H. M., 2012, The Astrophysical Journal, 758, L12
- Spergel D. N., Flauger R., Hložek R., 2015, Phys. Rev. D, 91, 023518
- Valentino E. D., Bouchet F. R., 2016, Journal of Cosmology and Astroparticle Physics, 2016, 011
- Valentino E. D., Melchiorri A., Silk J., 2019, Nature Astronomy

Weinberg S., 2008, Cosmology. Cosmology, OUP Oxford, https://books.google.cl/books?id=nqQZdg020fsC

Wu H.-Y., Huterer D., 2017, Monthly Notices of the Royal Astronomical Society, 471, 4946

Xu Y., Zhan H., Cheung Y.-K. E., 2019, Journal of Cosmology and Astroparticle Physics, 2019, 006

Yang W., Pan S., Mota D. F., 2017, Phys. Rev. D, 96, 123508

Yang W., Pan S., Valentino E. D., Nunes R. C., Vagnozzi S., Mota D. F., 2018, Journal of Cosmology and Astroparticle Physics, 2018, 019

Yuan W., Riess A. G., Macri L. M., Casertano S., Scolnic D. M., 2019, The Astrophysical Journal, 886, 61

Zhang J.-F., Geng J.-J., Zhang X., 2014, Journal of Cosmology and Astroparticle Physics, 2014, 044

Zhao M.-M., He D.-Z., Zhang J.-F., Zhang X., 2017, Phys. Rev. D, 96, 043520 Zhao M.-M., Zhang J.-F., Zhang X., 2018, Physics Letters B, 779, 473

APPENDIX A: COEFFICIENTS τ_I

The solutions for τ_i are

$$\tau_{1} = -1 + 2f_{0} \qquad (A1)$$

$$\tau_{2} = \frac{H_{0}^{\text{Pl}}}{2} - 2f_{0}H_{0}^{\text{Pl}} - f_{1} \qquad (A2)$$

$$\tau_{3} = \frac{1}{3} \left(2c^{2}f_{0}g_{2} - f_{0}H_{0}^{\text{Pl}^{2}}q^{\text{Pl}} + 2f_{0}H_{0}^{\text{Pl}^{2}}\right)$$

$$+ \frac{1}{6} \left(H_{0}^{\text{Pl}^{2}}q_{0}^{\text{Pl}} - H_{0}^{\text{Pl}^{2}}\right) \qquad (A3)$$

$$\tau_{4} = \frac{1}{12} \left(-8c^{2}f_{0}g_{2}H_{0}^{\text{Pl}} - 6c^{2}f_{1}g_{2} - 2f_{0}H_{0}^{\text{Pl}^{3}}j_{0}^{\text{Pl}}$$

$$+ 10f_{0}H_{0}^{\text{Pl}^{3}}q_{0}^{\text{Pl}} - 3f_{0}H_{0}^{\text{Pl}^{3}} + f_{1}H_{0}^{\text{Pl}^{2}}q_{0}^{\text{Pl}} - 2f_{1}H_{0}^{\text{Pl}^{2}}\right)$$

$$+ \frac{1}{24} \left(H_{0}^{\text{Pl}^{3}}j_{0}^{\text{Pl}} - 4H_{0}^{\text{Pl}^{3}}q_{0}^{\text{Pl}} + H_{0}^{\text{Pl}^{3}}\right) \qquad (A4)$$

$$\tau_{5} = \frac{1}{60} \left(24c^{4}f_{0}g_{4} + 4c^{2}f_{0}g_{2}H_{0}^{\text{Pl}^{2}}q_{0}^{\text{Pl}} + 8c^{2}f_{0}g_{2}H_{0}^{\text{Pl}^{2}}$$

$$- 6c^{2}f_{1}g_{2}H_{0}^{\text{Pl}^{4}} + 23f_{0}H_{0}^{\text{Pl}^{4}}j_{0}^{\text{Pl}} + 12f_{0}H_{0}^{\text{Pl}^{4}}q_{0}^{\text{Pl}^{2}}$$

$$- 35f_{0}H_{0}^{\text{Pl}^{4}}q_{0}^{\text{Pl}} + 2f_{0}H_{0}^{\text{Pl}^{4}} + 3f_{1}H_{0}^{\text{Pl}^{3}}j_{0}^{\text{Pl}}$$

$$- 13f_{1}H_{0}^{\text{Pl}^{3}}q_{0}^{\text{Pl}} - f_{1}H_{0}^{\text{Pl}^{3}}\right) + \frac{1}{120} \left(-7H_{0}^{\text{Pl}^{4}}j_{0}^{\text{Pl}}$$

$$- 4H_{0}^{\text{Pl}^{4}}q_{0}^{\text{Pl}^{2}} + 11H_{0}^{\text{Pl}^{4}}q_{0}^{\text{Pl}} - H_{0}^{\text{Pl}^{4}}\right) \qquad (A5)$$

This paper has been typeset from a TEX/LATEX file prepared by the author.